Progress In Electromagnetics Research, Vol. 120, 309–326, 2011

THEORETICAL STUDY OF MICROWAVE TRANSISTOR AMPLIFIER DESIGN IN THE CONJUGATELY CHARACTERISTIC-IMPEDANCE TRANSMISSION LINE (CCITL) SYSTEM USING A BILINEAR TRANSFORMATION APPROACH

R. Silapunt[1, *] and D. Torrungrueng[2]

[1]Department of Electronic and Telecommunication Engineering, Faculty of Engineering, King Mongkut's University of Technology Thonburi, Bangkok 10140, Thailand

[2]Department of Electrical and Electronic Engineering, Faculty of Engineering and Technology, Asian University, Chon Buri 20260, Thailand

Abstract—Conjugately characteristic-impedance transmission lines (CCITLs) are a class of transmission lines possessing conjugately characteristic impedances ($Z_0^{\pm}$) for waves propagating in the opposite direction. A typical Z_0 uniform transmission line is a special case of CCITLs whose argument of $Z_0^{\pm}$ is equal to 0°. This paper aims to generalize the CCITL system by demonstrating a theoretical study of CCITLs and their applications in the microwave transistor amplifier design. It is found that the bilinear transformation plays an important role in transforming circles in the reflection coefficient Γ_0-plane in the Z_0 system to the Γ-plane in the CCITL system. In addition, Meta-Smith charts, a graphical tool developed for solving problems in the CCITL system, are employed to design matching networks to achieve desired amplifier properties. Results show that stability regions on Meta-Smith charts can be determined, and source and load reflection coefficients can be selected properly to obtain desired operating power gain. In addition, an example shows that Meta-Smith charts offer a simple approach for matching network design using open-circuited single-stub shunt tuners.

Received 5 August 2011, Accepted 7 September 2011, Scheduled 20 September 2011

* Corresponding author: Rardchawadee Silapunt (rardchawadee.sil@kmutt.ac.th).

1. INTRODUCTION

Amplifiers operated in a high-frequency range ideally possess maximum gain, minimum noise figure, and low voltage standing wave ratio (VSWR), while being able to maintain their overall stability. Practical amplifier design, on the other hand, heavily relies on trade-offs and compromises as it inevitably involves integrating different sub-components with different characteristics. The graphical tool such as the Smith chart has then been developed for a graphical-aided design of high-frequency devices such as microwave amplifiers in the Z_0 system [1–3], where Z_0 is the characteristic impedance (usually with a real value) of a transmission line (TL) of interest. The mathematical expressions for the graphical solutions have been further formulated and optimized in an effort to achieve certain properties of amplifiers [4]. The typical approach in an amplifier design methodology involves a selection and tailoring of sub-components. In particular, a large community of researchers has paid a great attention to interconnects or TLs between these high-frequency sub-components as the TLs can greatly alter characteristics of the traveling signals and ultimately, the properties of amplifiers. TLs can typically be classified into several types such as reciprocal lossless and lossy TLs, nonreciprocal lossless [5–8] and lossy [2] TLs, and exponential tapered lossless nonuniform TLs [3, 9–11]. Some of these have already been employed for practical applications, while some novel ones have been modeled and fabricated; i.e., metamaterial TLs possessing negative refractive index and permeability [12–17]. Although the tremendous increase in wideband amplifiers has dramatically shifted the design methodology to focus more on the macro framework of wideband operation [18, 19], component selection and integration [20–22] are still viable approaches that can greatly improve the overall performance of amplifiers.

This paper discusses a theoretical study of one class of TLs, namely, the conjugately characteristic-impedance TLs (CCITLs) and their applications in the microwave transistor amplifier design. CCITLs are a class of TLs possessing conjugately characteristic impedances for waves propagating in opposite directions. Examples of lossless TLs listed above are considered as CCITLs since they exhibit CCITL characteristics. As pointed out in [7], a typical Z_0 uniform TL is a special case of CCITLs. Thus, it is interesting to generalize the amplifier design in the Z_0 system to that in the CCITL system. So far, it has been proved that CCITLs can be used effectively to analyze periodic TL structures whose applications include slow wave components, antenna, and metamaterials. However, their compatibility and performance when integrated to form microwave

transistor amplifiers have yet to be fully demonstrated.

Design problems involving typical Z_0 uniform TLs (e.g., matching network design) are generally carried out intuitively using the conventional graphical tool, the Smith chart. Recently, Torrungrueng and Thimaporn have proposed a novel graphical tool, called the Meta-Smith charts (previously known as the T-charts) [7], to analyze potential applications in the CCITL system [7, 9, 23, 24]. Note that Meta-Smith charts are a generalization of the Smith chart for CCITLs. For matching networks, Meta-Smith charts can be applied in several fashions, such as lump element tuning, single stub tuning, and double stub tuning [24]. However, in order to incorporate component parameters that are typically in the Z_0 system into the CCITL system, a rigorous mathematical derivation is necessary, for example, the derivation of S-parameter and power gain conversions. Therefore, the bilinear transformation [25], a graphical technique used to transform circles between complex planes, can be adopted to transform associated circles in the Γ_0-plane in the Z_0 system into those in the CCITL system. Note that many amplifier design problems deal with relevant circle equations at the great extent, e.g., stability circles, power gain circles, and noise circle.

The goal of this paper is to characterize and understand the CCITL system in more depth, especially with regard to its capability of integration to microwave amplifiers using the bilinear transformation technique associated with Meta-Smith charts. This paper is arranged in the following order. Section 2 presents the theory of CCITLs and Meta-Smith charts. Section 3 presents the general properties of CCITL two-port networks. Section 4 presents the bilinear transformation approach. Section 5 presents the application of the bilinear transformation approach to microwave transistor amplifier design, and Section 6 presents conclusions.

2. THEORY OF CCITLS AND META-SMITH CHARTS

In this section, only reciprocal CCITLs whose propagation constant β is the same for both forward and reverse directions are discussed. The traveling wave equations for the phasor voltage $V(z)$ and the phasor current $I(z)$ for a CCITL of length l, terminated in a load impedance Z_L as shown in Figure 1, can be written compactly as

$$V(z) = V^+ e^{-j\beta z} + V^- e^{j\beta z}, \tag{1}$$

$$I(z) = \frac{V^+}{Z_0^+} e^{-j\beta z} - \frac{V^-}{Z_0^-} e^{j\beta z}. \tag{2}$$

Note that V^+ and V^- in (1) and (2) are defined as the amplitudes of incident and reflected voltage waves referenced at $z = 0$, respectively. In (2), Z_0^+ and Z_0^- are defined as characteristic impedances of CCITLs entering and leaving the terminal (the terminal definition) respectively. Both values are complex conjugates of one another [7]. $Z_0^{\pm}$ can be defined as

$$Z_0^{\pm} \equiv |Z_0|\, e^{\mp j\phi}, \tag{3}$$

where $|Z_0|$ and ϕ are the absolute value and the argument of Z_0^-, respectively. In this paper, only nonnegative characteristic resistances (NNCRs) are considered; i.e., the argument ϕ must lie in the following range [24]:

$$-90^\circ \leq \phi \leq 90^\circ. \tag{4}$$

In addition to Figure 1, the total impedance seen at the input of the CCITL and the voltage reflection coefficient from the load are designated as Z_{IN} and Γ, respectively.

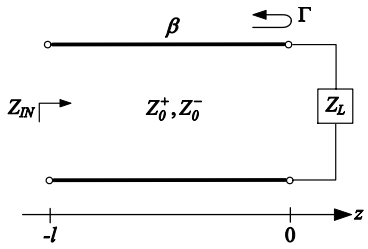

Figure 1. A reciprocal CCITL terminated in a passive load Z_L.

Analytical approaches for solving problems associated with CCITLs usually provide complex formulae [24]. To assist in the analysis and design of CCITLs, graphical tools can be useful. Graphical tools usually provide a more physical insight of visualizing associated CCITL phenomenon and solving related problems more effectively. Since 2004, Meta-Smith charts have been applied to CCITLs [7]. They are constructed using the same approach as in constructing the Smith chart. For the Meta-Smith chart for CCITLs with NNCRs, the region of interest is always inside or on the unit circle in the Γ-plane for passive load terminations [24]. It has been found that this Meta-Smith chart depends in a complicated fashion on the argument ϕ defined in (3). Mathematical details and applications of the Meta-Smith chart can be found in [24].

3. GENERAL PROPERTIES OF CCITL TWO-PORT NETWORKS

The different characteristics of the CCITL system and the Z_0 system result in different expressions of TL parameters and other parameters associated with the two-port device integration. Figure 2 illustrates a microwave transistor amplifier diagram in the CCITL system in which an input matching network (IMN) and an output matching network (OMN) are integrated for completeness. Note here that the designated $Z_0^{\mp}$ at the input side is used to represent CCITLs with Z_0^- and Z_0^+ leaving and entering the source terminal respectively, while $Z_0^{\pm}$ at the output side is used to represent CCITLs with Z_0^+ and Z_0^- entering and leaving the load terminal, respectively. Signal reflections in the two-port network (microwave transistor) occur at 4 different locations; i.e., source, input port (Port 1), output port (Port 2), and load as shown in Figure 2, where E_1, Z_1, and Z_2 are source voltage, source impedance, and desired load impedance, respectively. Note that the reflection coefficients are defined differently between the CCITL system and the Z_0 system due to the different characteristic impedances of CCITLs. The lengths l_1 and l_2 in Figure 2 represent CCITL lengths between the IMN and Port 1 and between the OMN and Port 2, respectively. As pointed out in [25], for standard TLs used in the Z_0 system, the two-port network can be treated as if CCITLs have zero length and have characteristic impedances Z_0^+ and Z_0^- connected at input and output ports.

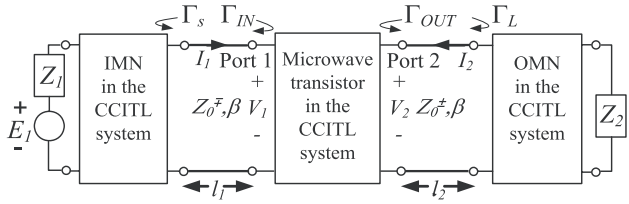

Figure 2. A microwave transistor amplifier diagram in the CCITL system.

By referring to the definition of incident and reflected waves stated previously in Section 2, mathematical expressions of relevant reflection coefficients can be found. First, the total voltage V_1 and current I_1 at the input port are related by the input impedance Z_{IN} as follows:

$$Z_{IN} \equiv \frac{V_1}{I_1}. \tag{5}$$

Using (1), (2), and (5) yields the voltage reflection coefficient at the

input port Γ_{IN} in the CCITL system in terms of associated impedances as

$$\Gamma_{IN} \equiv \frac{V_1^-}{V_1^+} = \frac{Z_{IN} Z_0^+ - Z_0^+ Z_0^-}{Z_{IN} Z_0^- + Z_0^+ Z_0^-}, \tag{6}$$

where V_1^+ and V_1^- are incident and reflected voltage waves at the input port, respectively. In addition, Figure 3 shows the Thévenin's equivalent circuit at the output port, where the output voltage reflection coefficient Γ_{OUT} in the CCITL system can be determined using a similar formulation to the input voltage reflection coefficient as

$$\Gamma_{OUT} \equiv \frac{V_2^-}{V_2^+} = \frac{Z_{OUT} Z_0^+ - Z_0^+ Z_0^-}{Z_{OUT} Z_0^- + Z_0^+ Z_0^-}, \tag{7}$$

where V_2^+ and V_2^- are incident and reflected voltage waves at the output port, respectively. In Figure 3, $E_{TH,OUT}$ and Z_{OUT} are the Thévenin's voltage and the Thévenin's impedance seen from the output port, respectively. The total load voltage V_L and current I_L are defined as the voltage across and the current flowing to the load impedance Z_L, where the OMN is included.

At the load, the total voltage V_L and the total current I_L are related by the load impedance Z_L as follows:

$$Z_L \equiv \frac{V_L}{I_L}. \tag{8}$$

Using (1), (2), and (8) yields the voltage reflection coefficient at the load Γ_L in the CCITL system in terms of associated impedances as

$$\Gamma_L \equiv \frac{V_L^-}{V_L^+} = \frac{Z_L Z_0^- - Z_0^+ Z_0^-}{Z_L Z_0^+ + Z_0^+ Z_0^-}, \tag{9}$$

where V_L^+ and V_L^- are incident and reflected voltage waves respectively, at the load as shown in Figure 3. Note that $V_L^{\pm} = V_2^{\mp}$ and $I_L = -I_2$ by

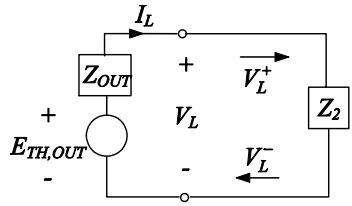

Figure 3. A Thévenin's equivalent circuit at the output port.

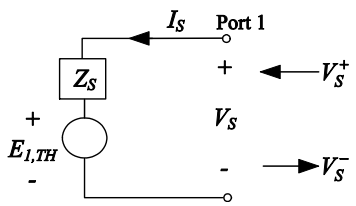

Figure 4. A Thévenin's equivalent circuit at the input port.

assuming zero length of the CCITL ($l_2 = 0$) in Figure 2. Furthermore, Figure 4 shows the Thévenin's equivalent circuit at the input port. With the Thévenin's voltage $E_{1,TH} = 0$, the total voltage V_S and the total current I_S at the input port are related by the source impedance Z_S (IMN is included) as follows:

$$Z_S \equiv \frac{V_S}{I_S}. \tag{10}$$

Using (1), (2), and (10), the voltage reflection coefficient at the source Γ_S in the CCITL system can be expressed as

$$\Gamma_S \equiv \frac{V_S^-}{V_S^+} = \frac{Z_S Z_0^- - Z_0^+ Z_0^-}{Z_S Z_0^+ + Z_0^+ Z_0^-}, \tag{11}$$

where V_S^+ and V_S^- are incident and reflected voltage waves respectively, at the source as shown in Figure 4. Note that $V_S^{\pm} = V_1^{\mp}$ and $I_S = -I_1$.

The difference between (6) and (11), which represent the input and source reflection coefficients respectively, is a result of the derivation following the definition of the CCITL traveling wave stated earlier. The relation of the output and load reflection coefficients in (7) and (9) respectively, appears in the same fashion. It should be pointed out that the forms of the input and output reflection coefficients are similar, and those of the source and load reflection coefficients are similar as well. Note that other expressions of reflection coefficients in the CCITL system than those shown above can be realized by considering different definitions of traveling wave in a two-port network such as those where the characteristic impedances Z_0^+ and Z_0^- are defined in the direction of entering and leaving ports respectively (the port definition) [26], and those where the traveling waves are defined based on the characteristic conductances of associated TLs [27, 28].

4. BILINEAR TRANSFORMATION APPROACH

The classic bilinear transformation or linear fraction transformation for a complex plane analysis [25] is applied here to map circles of interest in the Γ^0-plane (in the Z_0 system) onto those in the Γ-plane (in the CCITL system). This transformation of the form

$$w = f(z) = \frac{az + b}{cz + d} \tag{12}$$

is conformal across the entire complex plane, where w and z are variables in the original and target planes respectively, and a, b, c, and d are complex constants with $ad - bc \neq 0$.

For instance, a load reflection coefficient Γ_L^0 derived for a Z_0 system can be shown to be a function of the source impedance Z_L and the characteristic impedance Z_0 as [25]

$$\Gamma_L^0 = \frac{Z_L - Z_0}{Z_L + Z_0}. \tag{13}$$

Then, the load impedance in a two-port network is rewritten in terms of Γ_L^0 and Z_0 and subsequently substituted in (9), yielding the bilinear transformation of the load reflection coefficient in the Z_0 system to that in the CCITL system in the form of

$$\Gamma_L^0 = \frac{a\Gamma_L + b}{c\Gamma_L + d}, \tag{14}$$

where Γ_L represents the load reflection coefficient in the CCITL system. In (14), the complex constants are given as $a = (|Z_0| + Z_0^+)$, $b = (|Z_0| - Z_0^-)$, $c = (|Z_0| - Z_0^+)$, and $d = (|Z_0| + Z_0^-)$. Due to the fact that the source and load reflection coefficients are in similar form, (13) and (14) can be applied for the source reflection coefficient as well.

Several graphical solutions in the microwave transistor amplifier design are determined from circle equations that are algebraically manipulated using transistor and TL parameters. The circle in the Z_0 system that is located in the Γ^0-plane can be mapped into that in the CCITL system that is located in the Γ-plane using the following equations [25]:

$$C = \frac{r_0^2 c^* d - (a')^* b'}{|a'|^2 - r_0^2 |c|^2}, \tag{15}$$

$$r = \frac{r_0 |a'd - b'c|}{\left||a'|^2 - r_0^2 |c|^2\right|}, \tag{16}$$

where C and r are the center and radius of the associated circle in the Γ-plane respectively, r_0 is the radius of the circle in the Γ^0-plane, $a' = a - cC_0$ and $b' = b - dC_0$, where C_0 is the center of the circle in the Γ^0-plane, and the superscript '*' represents a complex conjugate. It is implicit from (14) that the bilinear transformation approach is altered by the argument ϕ of $Z_0^{\pm}$ and can also be applied in a backward direction to map circles in the Γ-plane onto those in the Γ^0-plane. This bilinear transformation offers a simpler and faster approach to systematically derive associated circle equations for microwave transistor amplifiers in the CCITL system compared to rigorous parameter conversions reported previously [26, 28].

5. APPLICATION OF THE BILINEAR TRANSFORMATION APPROACH TO MICROWAVE TRANSISTOR AMPLIFIER DESIGN IN THE CCITL SYSTEM

Ones of important components of the microwave transistor amplifier are the IMN and OMN that are usually implemented to ensure desired characteristics from source to input and from load to output, respectively. Reliable matching tools typically used are short-ended and open-ended circuit stubs [29–31] which are sections of the same type of TLs. Most important properties to be addressed in transistor amplifier design include stability, power gain, VSWR, and noise. Note that power gain can be categorized into three types: operating power gain G_P, transducer power gain G_T, and available power gain G_A. The graphical tool technically offers some flexibility in selecting a desired power gain for the amplifier by separating the design into two parts, one at the input using the available power gain and the other at the output using the operating power gain. The conjugate matches on both sides are in general not possible. Therefore, a designer usually defines a certain gain on one side to satisfy other properties and uses the conjugate match on the other. A series of mathematical manipulations finally provides sets of circle equations possessing certain properties [25]. Figure 5 shows a schematic diagram of the microwave transistor amplifier using reciprocal open-circuited single-stub shunt tuners as the IMN and OMN in the CCITL system. Similar to the Smith chart for the Z_0 system, Meta-Smith charts will be used extensively to design the amplifier in the CCITL system. Included in this section are the bilinear transformation for the CCITL system and the subsequent Meta-Smith chart approach to design matching

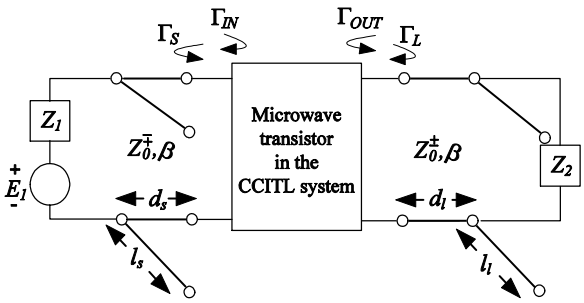

Figure 5. A schematic diagram of the microwave transistor amplifier using reciprocal open-circuited single-stub shunt tuners in the CCITL system for matching networks.

networks of the amplifier to achieve the desired properties of stability and power gain. Two operating types of transistors, unconditionally stable and potentially unstable, are studied. Results are compared with the design using the characteristic conductance (CC) approach associated with the port definition of characteristic impedances [32, 33].

5.1. Stability Considerations in the CCITL System

The stability of the microwave amplifier is one of the most important issues in the design. At a given frequency in the CCITL system, oscillations of the microwave transistor amplifier are possible when the input and/or output ports present a negative resistance resulting in $|\Gamma_{IN}| > 1$ and/or $|\Gamma_{OUT}| > 1$. To design an unconditionally stable amplifier in the CCITL system, the real parts of the input and output impedances, $\mathrm{Re}\{Z_{IN}\}$ and $\mathrm{Re}\{Z_{OUT}\}$ respectively, must be greater than zero for all passive load and source terminations.

The graphical solutions of the input and output stability circles (ISC and OSC, respectively) in the Z_0 system were previously derived [25]. Specifically, the center C_s^0 and the radius r_s^0 of the ISC are given as

$$C_s^0 = \frac{\left(S_{11}^0 - \Delta^0 S_{22}^{0*}\right)^*}{\left|S_{11}^0\right|^2 - \left|\Delta^0\right|^2}, \tag{17}$$

$$r_s^0 = \left|\frac{S_{12}^0 S_{21}^0}{\left|S_{11}^0\right|^2 - \left|\Delta^0\right|^2}\right|, \tag{18}$$

where S_{ij}^0 is the S-parameter of the transistor in the Z_0 system (i and j are equal to 1 and 2) and Δ^0 is defined as $S_{11}^0 S_{22}^0 - S_{12}^0 S_{21}^0$. By using the bilinear transformation, C_s^0 and r_s^0 in (17) and (18) are substituted as C_0 and r_0 respectively into (15) and (16) resulting in the center C_s and the radius r_s in the CCITL system, respectively. If a transistor is unconditionally stable, the ISC and OSC must lie outside both the Smith chart in the Z_0 system and Meta-smith charts in the CCITL system. For example, the values of $|C_s| - r_s$ after the bilinear transformation into the CCITL system of the ISC of the unconditionally stable transistor in the Z_0 system, Motorola MRF962, operated at 1.5 GHz, $V_{CE} = 10\,\mathrm{V}$, and $I_C = 10\,\mathrm{mA}$ with S-parameters given as follows: $S_{11}^0 = 0.77\,\underline{|168^\circ}$, $S_{12}^0 = 0.085\,\underline{|{+31}^\circ}$, $S_{21}^0 = 1.72\,\underline{|{+55}^\circ}$, and $S_{22}^0 = 0.31\,\underline{|{-104}^\circ}$, are found to be greater than 1 for every argument ϕ. These results indicate that all ISCs are located outside Meta-Smith charts in the Γ_S-plane, and the same results are obtained when calculating values of $|C_l| - r_l$ on the output side. Thus,

this transistor is unconditionally stable in the CCITL system, and all passive source and load terminations provide stable operation.

However, there may be some values of Γ_S and Γ_L for which the real parts of input and output impedances are negative resulting in a potentially unstable amplifier in the CCITL system. The graphical analysis can be used to evaluate these particular Γ_S and Γ_L values corresponding with associated regions in Meta-Smith charts. The values of Γ_{IN} and Γ_{OUT} can thus be determined accordingly, if S-parameters in the CCITL system are known, as shown in (19) and (20) respectively,

$$\Gamma_{IN} = S_{11} + \frac{S_{12}S_{21}\Gamma_L}{1 - S_{22}\Gamma_L}, \tag{19}$$

$$\Gamma_{OUT} = S_{22} + \frac{S_{12}S_{21}\Gamma_S}{1 - S_{11}\Gamma_S}. \tag{20}$$

By applying the bilinear transformation to the potentially unstable transistor, the ISC and OSC in the CCITL system can also be drawn in Meta-Smith charts. The stability of the amplifier is obtained when Γ_S and Γ_L values are chosen in stable regions that may be inside or outside stability circles depending on transistor characteristics. A test transistor NEC NE3210S01 is employed in this example to determine the stability for both input and output sides. The S-parameters of this test transistor in the $50\,\Omega$ system at the operating frequency $f = 2.4\,\text{GHz}$ are given as follows: $S_{11}^0 = 0.955\,\underline{\lfloor -26.4^\circ}$, $S_{12}^0 = 0.027\,\underline{\lfloor +72.14^\circ}$, $S_{21}^0 = 4.452\,\underline{\lfloor +148.5^\circ}$, and $S_{22}^0 = 0.54\,\underline{\lfloor -18.96^\circ}$. These S-parameters are then substituted in stability circle equations after which respective circles are plotted in the Γ-plane using the bilinear transformation approach. Figure 6 shows the ISC and the OSC in Meta-Smith charts at $\phi = -30^\circ$, 0°, and 30°. The unit constant resistance (r) and conductance (g) circles are denoted as $r = 1$ and $g = 1$, respectively. It is found that the stable regions, i.e., those located on Meta-Smith charts outside stability circles for this test transistor, increase with the argument ϕ for both input and output. However, this result requires a certain validation in order to interpret the relationship between stable regions and the level of stability correctly. Thus, the bilinear transformation is applied in a backward direction to map the ISC and the OSC in Meta-Smith charts for $\phi \neq 0^\circ$ to the corresponding circles with $\phi = 0^\circ$ (or the Smith chart). It is found that the sizes and locations of the mapped ISC and OSC are identical to those determined in the Z_0 system using (17) and (18). These results imply that the stability does not vary with the argument ϕ, and the generalization of the stability for the Z_0 system to that for $\phi \neq 0^\circ$ in the CCITL system is successfully performed.

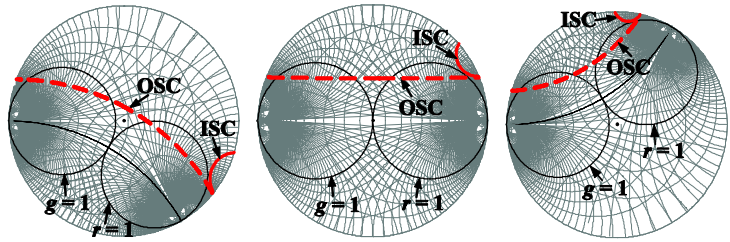

Figure 6. ISC and OSC are plotted on Meta-Smith charts using solid and dashed lines respectively for (a) $\phi = -30°$, (b) $\phi = 0°$, and (c) $\phi = 30°$.

It is found next that both Meta-Smith chart and its corresponding stability circles at $\phi = 0°$ for both unconditionally stable and potentially unstable test transistors appear to be similar to those determined using the CC approach associated with the port definition used in [32, 33], respectively; however for the case where $\phi \neq 0°$, the terminal definition of the characteristic impedances $Z_0^{\pm}$ results in different presentations of Meta-Smith charts and their corresponding stability circles. In particular, Meta-Smith charts derived using the terminal definition at a certain argument ϕ appear similar to those derived using the port definition at the same magnitude of the argument ϕ but with the opposite sign.

5.2. Operating Power Gain Considerations in the CCITL System

The same test transistor is used to derive graphical solutions for the operating power gain G_P circle in the Z_0 system [25]. The G_P circle in the Γ_L^0-plane is then mapped onto the corresponding circle in Meta-Smith charts in the Γ_L-plane as shown in Figure 7 for $G_P = 15$ dB for $\phi = -30°$, $0°$, and $30°$. The operating power gain can be found in terms of S-parameters and the load reflection coefficient in the CCITL system as

$$G_P \equiv \frac{P_L}{P_{IN}} = \frac{1}{\left(1 - |\Gamma_{IN}|^2\right)} |S_{21}|^2 \frac{1 - |\Gamma_L|^2}{|1 - S_{22}\Gamma_L|^2}, \tag{21}$$

where P_L is the power delivered to the load and P_{IN} is the power at the input port. As was true of the stability circles derived earlier, the location and size of the mapped power gain G_P circle at $\phi = 0°$ using the bilinear transformation approach associated with the terminal definition is consistent with that derived using the CC approach associated with the port definition and the Z_0 system. This finding

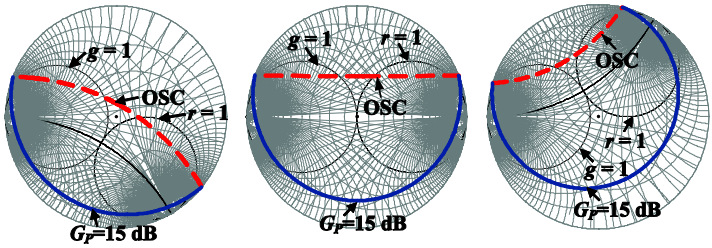

(a) (b) (c)

Figure 7. Operating power gain circle (solid line) of 15 dB derived using the bilinear transformation approach at (a) $\phi = -30°$, (b) $\phi = 0°$, and (c) $\phi = 30°$.

fits our expectations. The difference of the results from the CC approach associated with the port definition for mapped circles at $\phi \neq 0°$ can again be explained by different definitions of the characteristic impedances.

5.3. Matching Network Design in the CCITL System

A matching circuit is another important component of the amplifier design to ensure desired amplifier characteristics. The difficulties with lump element implementation and the inflexibility of quarter-wave lines suggest that stub matching is a better choice in microwave circuit matching. The matching circuit configuration designed for the test potentially unstable amplifier on Meta Smith-charts employs reciprocal CCITL open-circuited single-stub shunt tuners as shown in Figure 5. The design parameters, d_s and d_l, are distances from the stub to the input and output ports respectively, and l_s and l_l are stub lengths associated with the input and output ports, respectively.

A design to achieve high stability and desired operating power gain of the amplifier in the CCITL system is demonstrated through a sample matching circuit by using the same potentially unstable transistor from the previous section. Figure 2 is used as an example of the final amplifier circuit, where Z_1, Z_2, and $|Z_0|$ are set equally to 50 Ω. First, the Γ_L value at each argument ϕ is selected on the 15 dB G_P circle (e.g., those shown in Figure 7) such that the highest stability can be obtained; i.e., the selected Γ_L value is located farthest away from the OSC. It should be pointed out that this 15 dB gain value is certainly below the maximum stable gain of 22 dB of this transistor [25]. In addition, the Γ_S values computed for a conjugate match ($\Gamma_S = \Gamma_{IN}^*$) are found to lie outside their respective ISCs for every argument ϕ indicating that the stability of the amplifier is obtained. The overall

stability of the amplifier is evaluated by the total input and output loop resistances, $R_S + R_{IN}$ and $R_L + R_{OUT}$, respectively. Figure 8 shows the plot of the total input and output loop resistances as a function of the argument ϕ. It is clear that both loop resistances are greater than zero over the test range of the argument ϕ. Therefore, the test amplifier with selected Γ_S and Γ_L values is stable.

Figure 9 shows one of the design solutions for the IMN on a Meta-Smith chart at the conjugate match condition ($\Gamma_S = \Gamma_{IN}^*$), which lies outside the ISC, at $\phi = 30°$ using the open-circuited single-stub arrangement illustrated in Figure 5. The input stub with length l_s and respective normalized input susceptance of b is placed across the normalized source impedance z_1 to obtain the normalized admittance of $y = 1+jb$ at point A on the constant $|\Gamma_S|$ circle in the Meta-Smith chart. Then, the TL with length d_s is connected in series for a conjugate match at the input port (Port 1). Note that SC and OC in Figure 9 represent shorted- and opened- circuit locations, respectively. Table 1 shows the coefficient values with respect to the wavelength λ_ϕ of the input stub length, l_s, and the distance to Port 1, d_s, which are designated as c_l and c_d respectively, from $\phi = -60°$ to $\phi = 75°$. Note that the actual stub length and distance depend on the wavelength λ_ϕ, where λ_ϕ is generally a function of the argument ϕ and varies depending on the type of CCITL [24]. The effects of the argument ϕ on the input stub length and the distance to Port 1 shown in this design can thus be realized by multiplying these coefficients with λ_ϕ when the specific CCITL is used. Similarly, the OMN can also be designed.

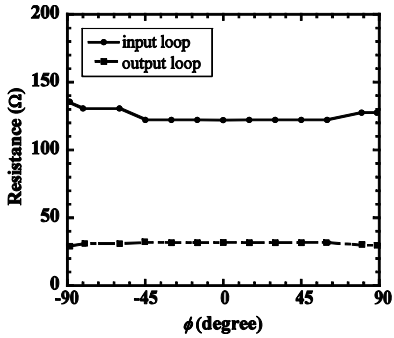

Figure 8. Total input and output loop resistances of the designed amplifier are plotted as a function of the argument ϕ with $G_P = 15\,\text{dB}$ and input conjugate matching.

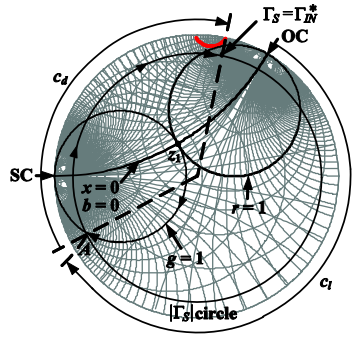

Figure 9. Meta-Smith chart solution using reciprocal CCITL open-circuited single-stub shunt tuners for the IMN at $\phi = 30°$.

Table 1. Coefficients for the stub length and the distance between the stub and Port 1 for input conjugate matching network.

ϕ (°)	c_l	c_d
−60	0.0599	0.4189
−45	0.0983	0.3780
−30	0.1299	0.3369
0	0.2122	0.2537
30	0.3036	0.1696
45	0.3517	0.1272
60	0.4006	0.0849
75	0.4501	0.0425

6. CONCLUSIONS

This paper demonstrates that, CCITLs can theoretically be integrated into a two-port network, e.g., transistors, to build microwave transistor amplifiers in the CCITL system using the bilinear transformation approach. It is shown that this approach can be effectively employed to transform stability and operating power gain circles in the Γ_0-plane into respective circles in the Γ-plane in the CCITL system, where Meta-Smith charts are effectively applied for associated matching network design. The generalization of the CCITL system is illustrated by the fact that the stability of the test transistor is independent of the argument ϕ. It is found that the CCITL amplifier can effectively maintain its stability and achieve desired operating power gain by interconnecting matching networks using reciprocal CCITL open-circuited single-stub shunt tuners whose length and distance depend on the wavelength λ_ϕ. Future work will include a further study, with Meta-Smith charts as an aided-design tool, on other design characteristics of the CCITL amplifier, e.g., noise and VSWR, including the practical implementation and characterization of CCITLs using periodic structures, and the implementation of novel CCITL amplifiers.

REFERENCES

1. Smith, P. H., *Electronic Applications of the Smith Chart*, NoblePublishing, Georgia, 2000.

2. Wu, Y., H. Y. Huang, and Y. N. Liu, "An extended omnipotent Smith chart with active parameters," *Microwave and Optical Technology Letters*, Vol. 50, No. 4, 896–899, 2008.
3. Wu, Y. and Y. Liu, "Standard Smith chart approach to solve exponential tapered nonuniform transmission line problems," *Journal of Electromagnetic Waves and Applications*, Vol. 22 No. 11–12, 1639–1646, 2008.
4. Roy, N. and V. K. Devabhaktuni, "A new computer aided LNA design approach targeting constant noise-figure and maximum gain," *PIERS Online*, Vol. 3, No. 8, 1321–1325, 2007.
5. Lindell, I. V., M. E. Valtonen, and A. H. Sihvola, "Theory of nonreciprocal and nonsymmetric uniform transmission lines," *IEEE Transactions on Microwave Theory and Techniques*, Vol. 42, No. 2, 291–297, 1994.
6. Lindell, I. V. and A. H. Sihvola, "Duality transformation for nonreciprocal and nonsymmetric transmission lines," *IEEE Transactions on Microwave Theory and Techniques*, Vol. 45, No. 1, 129–131, 1997.
7. Torrungrueng, D. and C. Thimaporn, "A generalized ZY Smith chart for solving nonreciprocal uniform transmission-line problems," *Microwave and Optical Technology Letters*, Vol. 40, No. 1, 57–61, 2004.
8. Hosseini, F., M. Khalaj-Amir Hosseini, and M. Yazdani, "A miniaturized Wilkinson power divider using nonuniform transmission line," *Journal of Electromagnetic Waves and Applications*, Vol. 23, No. 7, 917–924, 2009.
9. Torrungrueng, D. and C. Thimaporn, "Application of the T-chart for solving exponentially tapered lossless nonuniform transmission-line problems," *Microwave and Optical Technology Letters*, Vol. 45, No. 5, 402–406, 2005.
10. Pozar, D. M., *Microwave Engineering*, 3rd edition, John Wiley & Sons, New Jersey, 2005.
11. Khalaj-amirhosseini, M., "Analysis of coupled nonuniform transmission lines using short exponential or linear sections," *Journal of Electromagnetic Waves and Applications*, Vol. 21, No. 3, 299–312, 2007.
12. Sanada, A., C. Caloz, and T. Itoh, "Characteristics of the composite right/left-handed transmission lines," *IEEE Microwave and Wireless Components Letters*, Vol. 14, No. 2, 68–70, Nov. 2004.

13. Horii, Y., C. Caloz, and T. Itoh, "Super-compact multilayered left-handed transmission line and diplexer application," *IEEE Transactions on Microwave Theory and Techniques*, Vol. 53, No. 4, 1527–1534, Apr. 2005.
14. Antonini, G., "A general framework for the analysis of metamaterial transmission lines," *Progress In Electromagnetics Research B*, Vol. 20, 353–373, 2010.
15. Wang, W., C. Liu, L. Yan, and K. Huang, "A novel power divider based on dual-composite right/left handed transmission line," *Journal of Electromagnetic Waves and Applications*, Vol. 23, No. 8–9, 1173–1180, 2009.
16. Mirzavand, R., B. Honarbakhsh, A. Abdipour, and A. Tavakoli, "Metamaterial-based phase shifters for ultra wide-band applications," *Journal of Electromagnetic Waves and Applications*, Vol. 23, No. 11–12, 1489–1496, 2009.
17. Choi, J. and C. Seo, "High-efficiency wireless energy transmission using magnetic resonance based on negative refractive index metamaterial," *Progress In Electromagnetics Research*, Vol. 106, 33–47, 2010.
18. Güne, F. and C. Bilgin, "A generalized design procedure for a microwave amplifier: A typical application example," *Progress In Electromagnetics Research B*, Vo. 10, 1–19, 2008.
19. Demirel, S., F. Gunes, and U. Ozkaya, "Design of an ultra-wideband, low-noise, amplifier using a single transistor: A typical application example," *Progress In Electromagnetics Research B*, Vol. 16, 371–387, 2009.
20. Russo, I., L. Boccia, G. Amendola, and G. Di Massa, "Simplified design flow of quasi-optical slot amplifiers," *Progress In Electromagnetics Research*, Vol. 96, 347–359, 2009.
21. Yoon, J., H. Seo, I. Choi, and B. Kim, "Wideband LNA using a negative gm cell for improvement of linearity and noise figure," *Journal of Electromagnetic Waves and Applications*, Vol. 24, No. 5–6, 619–630, 2010.
22. Lee, M.-W., S.-H. Kam, Y.-S. Lee, and Y.-H. Jeong, "A highly efficient three-stage Doherty power amplifier with flat gain for WCDMA applications," *Journal of Electromagnetic Waves and Applications*, Vol. 24, No. 17–18, 2537–2545, 2010.
23. Torrungrueng, D. and S. Lamultree, "Equivalent graphical solutions of terminated conjugately characteristic impedance transmission lines with non-negative and corresponding negative characteristic resistances," *Progress In Electromagnetics Research*, Vol. 92, 137–151, 2009.

24. Torrungrueng, D., *Meta-Smith Charts and Their Potential Applications*, Morgan and Claypool, California, 2010.
25. Gonzalez, G., *Microwave Transistor Amplifiers*, 2nd edition, Prentice-Hall, New Jersey, 1997.
26. Silapunt, R. and D. Torrungrueng, "An analysis of two-port networks in the system of conjugately characteristic-impedance transmission lines (CCITLs)," *Proc. of the 2005 EECON Conference*, Phuket, Thailand, 2005.
27. Zappelli, L., "On the definition of the generalized scattering matrix of a lossless radial line," *IEEE Trans. Microwave Theory Tech.*, Vol. 52, No. 6, 1654–1662, 2004.
28. Silapunt, R. and D. Torrungrueng, "A comparison of two-port network in the CCITL system," *IEEE AP-S International Symposium*, 1197–1200, New Mexico, USA, 2006.
29. Heidari, A. A., M. Heyrani, and M. Nakhkash, "A dual-band circularly polarized stub loaded microstrip patch antenna for GPS applications," *Progress In Electromagnetics Research*, Vol. 92, 195–208, 2009.
30. Li, X., Y.-J. Yang, L. Yang, S.-X. Gong, T. Hong, X. Chen, Y.-J. Zhang, X. Tao, Y. Gao, K. Ma, and X.-L. Liu, "A novel unequal Wilkinson power divider for dual-band operation," *Journal of Electromagnetic Waves and Applications*, Vol. 24, No. 8–9, 1012–1022, 2010.
31. Li, J. C., J. C. Nan, X. Y. Shan, and Q. F. Yan, "A novel modified dual-frequency Wilkinson power divider with open stubs and optional isolation," *Journal of Electromagnetic Waves and Applications*, Vol. 24, No. 16, 2223–2235, 2010.
32. Silapunt, R. and D. Torrungrueng, "Stability considerations for the design of microwave transistor amplifiers in the CCITL system," *Proc. of the 2006 ECTI-CON*, 115–118, Ubon Ratchatani, Thailand, 2006.
33. Silapunt, R. and D. Torrungrueng, "Stability considerations of potentially unstable broadband microwave transistor amplifiers in the CCITL system," *Mediterranean Microwave Symposium*, 261–264, Budapest, Hungary, 2006.